

EXPLORING THE HELIUM CORE OF THE δ SCUTI STAR COROT 102749568 WITH ASTEROSEISMOLOGY

XINGHAO CHEN^{1,2,3}, YAN LI^{1,2,3,4}, GUIFANG LIN^{1,2}, YANHUI CHEN^{2,5,6}, AND JUNJUN GUO^{1,2,3}

Draft version September 19, 2021

ABSTRACT

Based on regularities in rotational splittings, we seek possible multiplets for the observed frequencies of CoRoT 102749568. Twenty-one sets of multiplets are identified, including four sets of multiplets with $l = 1$, nine sets of multiplets with $l = 2$, and eight sets of multiplets with $l = 3$. In particular, there are three complete triplets (f_{10}, f_{12}, f_{14}) , (f_{31}, f_{34}, f_{35}) , and (f_{41}, f_{43}, f_{44}) . The rotational period of CoRoT 102749568 is estimated to be $1.34^{+0.04}_{-0.05}$ days. When doing model fittings, three $l = 1$ modes (f_{12} , f_{34} , and f_{43}) and the radial first overtone f_{13} are used. Our results shows that the three nonradial modes (f_{12} , f_{34} , and f_{43}) are mixed modes, which mainly provide constraints on the helium core. The radial first overtone f_{13} mainly provides constraint on the stellar envelope. Hence the size of the helium core of CoRoT 102749568 is determined to be $M_{\text{He}} = 0.148 \pm 0.003 M_{\odot}$ and $R_{\text{He}} = 0.0581 \pm 0.0007 R_{\odot}$. The fundamental parameters of CoRoT 102749568 are determined to be $M = 1.54 \pm 0.03 M_{\odot}$, $Z = 0.006$, $f_{\text{ov}} = 0.004 \pm 0.002$, $\log g = 3.696 \pm 0.003$, $T_{\text{eff}} = 6886 \pm 70$ K, $R = 2.916 \pm 0.039 R_{\odot}$, and $L = 17.12 \pm 1.13 L_{\odot}$.

Subject headings: Rotational splitting; δ Scuti star; Optimal model; Helium core; CoRoT 102749568

1. INTRODUCTION

Thanks to the space missions, MOST (Walker et al. 2003), CoRoT (Baglin et al. 2006), and *Kepler* (Borucki et al. 2010), many δ Scuti stars are observed precisely (e.g., HD 144277 (Zwintz et al. 2011), HD 50844 (Poretti et al. 2009), and KIC 9700322 (Breger et al. 2011)). In particular, a large number of pulsation frequencies are detected in the light curves of some δ Scuti stars, such as HD 174936 (García Hernández et al. 2009), HD 50870 (Mantegazza et al. 2012), and HD 174966 (García Hernández et al. 2013). Due to the complexity of the frequency content, it is very difficult to disentangle the whole spectra of δ Scuti stars. Recently, Paparó et al. (2016) developed a sequence search method, and found a large number of series of quasi-equally spaced frequencies in 77 δ Scuti stars. Besides, Chen et al. (2016) attempted to interpret the frequency spectra of the δ Scuti star HD 50844 using the rotational splitting.

CoRoT 102749568 was observed from 24 October 2007 to 3 March 2008 ($\Delta T = 131$ days) by CoRoT during the first long run in the anti-centre direction (LRa01). Guenther et al. (2012) classified the δ Scuti star CoRoT 102749568 as an F1 IV star on the basis of the low-resolution $R = 1300$ spectra, which were observed in January 2009 with AAOmega multi-object spectrograph mounted on Anglo-Australian 3.9-m Telescope.

Paparó et al. (2013) converted the spectral type F1 IV of CoRoT 102749568 into effective temperature T_{eff} and gravitational acceleration $\log g$ using the calibrated values from Strazys & Kuriliene (1981), and then obtained $T_{\text{eff}} = 7000 \pm 200$ K and $\log g = 3.75 \pm 0.25$ by means of fitting AAOmega

spectra with stellar atmosphere models of Kurucz (Kurucz 1979). Moreover, Paparó et al. (2013) obtained $v \sin i = 115 \pm 20$ km s⁻¹ from the high-resolution $R = 85000$ spectra, which were observed with Mercator Echelle Spectrograph mounted on 1.2-m Mercator Telescope of Roque de los Muchachos Observatory. Furthermore, Paparó et al. (2013) extracted a total of 52 independent pulsation frequencies from the CoRoT timeseries. These frequencies are listed in Table 1. They identified the oscillation frequency 9.702 d⁻¹ with the largest amplitude as the radial first overtone with the method of multi-colour photometry. Moreover, Paparó et al. (2013) identified other 11 frequencies based on the regularities in frequency spacings.

Mode identification is very important for the asteroseismic study of pulsation stars. For a rotating star, the regularities due to rotational splitting in observed frequencies help us much to identify their spherical harmonic degree l and azimuthal number m . Based on the rotational splitting law of g modes, we successfully disentangled the frequency spectra of the δ Scuti star HD 50844 (Chen et al. 2016). That motivates us to analyze another δ Scuti star CoRoT 102749568 with the same method. In Section 2, we propose our mode identification by means of rotational splitting. In Section 3, we describe the details of input physics and model calculations. Input physics are described in Section 3.1, model grids are elaborated in Section 3.2, and the optimal model are analyzed in Section 3.3. We discuss our results in Section 4, and summarize the results in Section 5.

2. MODE IDENTIFICATION BASED ON ROTATIONAL SPLITTING

A pulsation mode is characterized by three indices, i.e., the radial order k , the spherical harmonic degree l , and the azimuthal number m (Christensen-Dalsgaard 2003). The azimuthal number m are degenerate for a spherically symmetric star. Namely, modes with the same k and l but different m have the same frequency. Stellar rotation will break the structure of spherical symmetry and result in frequency splitting, i.e., one nonradial pulsation frequency will split into $2l + 1$ different frequencies. According to the theory of stellar oscillation, a general formula for rotational splitting is described

¹ Yunnan Observatories, Chinese Academy of Sciences, P.O. Box 110, Kunming 650011, China; chenxinghao@ynao.ac.cn; ly@ynao.ac.cn

² Key Laboratory for Structure and Evolution of Celestial Objects, Chinese Academy of Sciences, P.O. Box 110, Kunming 650011, China

³ University of Chinese Academy of Sciences, Beijing 100049, China

⁴ Center for Astronomical Mega-Science, Chinese Academy of Sciences, 20A Datun Road, Chaoyang District, Beijing, 100012, China

⁵ Institute of Astrophysics, Chuxiong Normal University, Chuxiong 675000, China

⁶ School of Physics and Electronical Science, Chuxiong Normal University, Chuxiong 675000, China

as (Aerts et al. 2010)

$$\nu_{k,l,m} = \nu_{k,l} + \beta_{k,l} \frac{m}{P_{\text{rot}}}. \quad (1)$$

In Equation (1), $\beta_{k,l}$ is the rotational parameter measuring the size of rotational splitting and P_{rot} the rotational period. For high-degree or high-order p modes, $\beta_{k,l} \simeq 1$. Values of rotational splitting for pulsation modes with different spherical harmonic degree l are the same. For high-order g modes, $\beta_{k,l} \simeq 1 - \frac{1}{l(l+1)}$ (Brickhill 1975). The rotational splitting derived from $l = 1$ modes and those from $l = 2$ modes and $l = 3$ modes conform to the relation $\delta\nu_{k,l=1} : \delta\nu_{k,l=2} : \delta\nu_{k,l=3} = 0.6 : 1 : 1.1$ (Winget et al. 1991). Based on these regularities in rotational splittings, we analyze the frequency spectra of CoRoT 102749568 and list possible multiplets in Table 2.

It can be noticed in Table 2 that we find twenty-one sets of multiplets, including three different types of rotational splitting. The averaged frequency splitting $\delta\nu_1$ is $4.451 \mu\text{Hz}$ for Multiplet 1, 2, 3, and 4. The averaged frequency splitting $\delta\nu_2$ is $7.453 \mu\text{Hz}$ for Multiplet 5, 6, 7, 8, 9, 10, 11, 12, and 13, and the averaged frequency splitting $\delta\nu_3$ is $8.176 \mu\text{Hz}$ for Multiplet 14, 15, 16, 17, 18, 19, 20, and 21. For these frequency differences in Table 2, we find that some of them approximate to the corresponding averaged value $\delta\nu_1$, $\delta\nu_2$, or $\delta\nu_3$ (e.g., Multiplet 1, 2, 3, and 5), and some of them are several times that of the corresponding average value (e.g., Multiplet 4, 11, 12, and 13). Moreover, we find that the ratio of $\delta\nu_1 : \delta\nu_2 : \delta\nu_3$ is $0.597 : 1.0 : 1.097$, which agrees well with the property of g modes. As shown in Figure 1, the δ Scuti star CoRoT 102749568 is in the post-main-sequence evolution stage with a contracting helium core and an expanding envelope. Such stellar structure may reproduce these behaviors of rotational splitting.

Based on the property of rotational splitting for g modes, we identify frequencies in Multiplet 1, 2, 3, and 4 as $l = 1$ modes, frequencies in Multiplet 5, 6, 7, 8, 9, 10, 11, 12, and 13 as $l = 2$ modes, and frequencies in Multiplet 14, 15, 16, 17, 18, 19, 20, and 21 as $l = 3$ modes. Furthermore, we find that the azimuthal number m of pulsation modes in Multiplet 1, 2, 3, 4, 6, and 13 can be uniquely identified, and the azimuthal number m of pulsation modes in other multiplets allow of several possibilities (e.g., three possibilities for pulsation modes in Multiplet 5).

Finally, there are three unidentified frequencies f_4 , f_{40} , and f_{52} , which do not show frequency splitting. Frequencies f_4 and f_{10} have a difference of $29.789 \mu\text{Hz}$, about four times that of $\delta\nu_{k,l=2}$. However, f_{10} has been regarded as one component of Multiplet 1. Multiplet 1 consists of three components, being a complete triplet. Frequencies f_{10} and f_{12} have a difference of $4.485 \mu\text{Hz}$, which agree well with the difference $4.399 \mu\text{Hz}$ between f_{12} and f_{14} . Besides, modes with lower degree l are easier to be observed because of the effect of geometrical cancellation. Frequencies f_{27} and f_{40} have a difference of $48.847 \mu\text{Hz}$, about six times that of $\delta\nu_{k,l=3}$. Similarly, the frequency f_{27} has been identified as one component of Multiplet 14. Frequencies f_{48} and f_{51} have a difference $29.712 \mu\text{Hz}$, about four times that of $\delta\nu_{k,l=2}$. Frequencies f_{48} and f_{52} have a difference of $40.597 \mu\text{Hz}$, about five times that of $\delta\nu_{k,l=3}$. The spherical harmonic degree of f_{48} allows of two possibilities, $l = 2$ or $l = 3$. For the former case, the azimuthal number m of f_{48} and f_{51} are determined to be $m = (-2, +2)$. This case is listed in Table 2. The azimuthal number of the latter case allows of two possibilities, i.e., $m =$

$(-3, +2)$ and $(-2, +3)$.

Based on the above analyses, the detection of triplets, quintuplets, and septuplets helps us to identify four sets of multiplets with $l = 1$, nine sets of multiplets with $l = 2$, and eight sets of multiplets with $l = 3$. Owing to the deviations from the asymptotic expression, we find in Table 2 that slight differences of the rotational splitting exist in different multiplets (e.g., in Multiplet 8 and 9). Besides, slight differences also exist in the same multiplet (e.g., in Multiplet 1). Furthermore, we find in Table 2 that there are only two components in Multiplet 4, 7, 8, 9, 10, 11, 12, 13, 15, 16, 17, 18, 19, 20, and 21. Different physical origins are also possible, such as the large separation led by the so-called island modes (García Hernández et al. 2013; Lignières et al. 2006) and the phenomenon of avoided crossings (Aizenman et al. 1977). The δ Scuti star CoRoT 102749568 is a slightly evolved star, the occurrence of avoided crossings will make the frequency spectra more complex. From the observed frequency spectra of CoRoT 102749568, it is difficult to find the signs of avoided crossings. Hence the phenomenon of avoided crossings is not considered in our work.

3. INPUT PHYSICS AND MODEL CALCULATIONS

3.1. Input physics

All of our theoretical models are computed with the Modules for Experiments in Stellar Astrophysics (MESA), which is developed by Paxton et al. (2011, 2013). We use the so-called module pulse from version 6596 to calculate stellar evolutionary models and their corresponding pulsation frequencies (Christensen-Dalsgaard 2008; Paxton et al. 2011, 2013).

In our calculations, the OPAL opacity table GS98 (Grevesse & Sauval 1998) series are adopted. We use the $T - \tau$ relation of Eddington grey atmosphere in the atmosphere integration, and choose the mixing-length theory (MLT) of Böhm-Vitense (1958) to treat convection. Based on numerical calculations, we find that theoretical evolutionary models are not sensitive to the mixing-length parameter. However, the values of $\beta_{k,l}$ of theoretical models with slightly higher α_{MLT} agree better with asymptotic values of g modes, hence $\alpha_{\text{MLT}} = 2.2$ is adopted in our work. Moreover, we find that theoretical models without convective core overshooting can not reproduce those observed multiplets. Hence we introduce the convective core overshooting in our calculations. For the overshooting mixing of the convective core, we adopt an exponentially decaying prescription. Following Freytag et al. (1996) and Herwig (2000), we introduce an overshoot mixing diffusion coefficient

$$D_{\text{ov}} = D_0 \exp\left(\frac{-2z}{f_{\text{ov}} H_p}\right). \quad (2)$$

In Equation (2), D_0 is the convective mixing coefficient, z the distance into radiative zone away from the boundary of convective core, H_p the pressure scale height, and f_{ov} an adjustable parameter describing the efficiency of the overshooting mixing. In our calculations, we set the lower limit of the diffusion coefficient $D_{\text{ov}}^{\text{limit}} = 1 \times 10^{-2} \text{ cm}^2/\text{s}$, below which no element mixing is allowed. In addition, effects of rotation and element diffusion are not considered in our work.

3.2. Model grids

The internal structure and the evolutionary track of a star depend on the initial mass M , the initial chemical composition (X, Y, Z) , and the overshooting parameters f_{ov} . A grid

of theoretical models are computed with MESA, M varying from $1.5 M_{\odot}$ to $2.2 M_{\odot}$ with a step of $0.01 M_{\odot}$, Z varying from 0.005 to 0.030 with a step of 0.001, and f_{ov} varying from 0 to 0.016 with a step of 0.001. In our calculations, we choose the initial helium fraction $Y = 0.245 + 1.54Z$ (e.g., Dotter et al. 2008; Thompson et al. 2014; Tian et al. 2015) as a function of mass fraction of heavy-elements Z .

Theoretical models for each star are computed from the zero-age main sequence to post-main-sequence stage. The error box in Figure 1 corresponds to the observed stellar parameters, i.e., the effective temperature $6800 \text{ K} < T_{\text{eff}} < 7200 \text{ K}$ and the gravitational acceleration $3.50 < \log g < 4.00$. We calculate frequencies of oscillation modes with $l = 0, 1, 2$, and 3 for every stellar model which falls inside the error box along the evolutionary track.

3.3. Optimal models

We try to use theoretical oscillation frequencies derived from a grid of evolutionary models to fit those of identified pulsation modes. According to the analyses in Section 2, mode identifications are unique only in Multiplet 1, 2, and 3 and their $m = 0$ components are observed. When doing model fittings, we hence use four identified pulsation modes, i.e., three $l = 1$ modes (f_{12} , f_{34} , and f_{43}) and the radial first overtone f_{13} . Paparó et al. (2013) identify the frequency f_{13} with the largest amplitude as the radial first overtone with the method of multi-colour photometry. In our calculations, we use the identification of f_{13} as the radial first overtone. When doing model fittings, we use the following criterion

$$\chi^2 = \frac{1}{n} \sum (|\nu_i^{\text{obs}} - \nu_i^{\text{theo}}|^2), \quad (3)$$

where ν_i^{obs} is the observed frequency, ν_i^{theo} the theoretically calculated frequency, and n the amount of the observed frequencies.

Figure 2 shows the plot of $1/\chi^2$ to the effective temperature T_{eff} for all theoretical models. Each curve in Figure 2 corresponds to one theoretical evolutionary track. In Figure 2, the filled circles correspond to seven candidate models of CoRoT 102749568 in Table 3.

Christensen-Dalsgaard (2003) defines the general expression of the rotational parameter $\beta_{k,l}$ of a pulsation mode for a rigid body as

$$\beta_{k,l} = \frac{\int_0^R (\xi_r^2 + L^2 \xi_h^2 - 2\xi_r \xi_h - \xi_h^2) r^2 \rho dr}{\int_0^R (\xi_r^2 + L^2 \xi_h^2) r^2 \rho dr}, \quad (4)$$

where the subscripts "r" and "h" correspond to the radial displacement and the horizontal displacement, ρ denotes the local density, and $L^2 = l(l+1)$. Based on the asymptotic behavior of the eigenfunctions of high-order g modes, $\beta_{k,l}$ can be simplified as being the asymptotic value $1 - \frac{1}{L^2}$. According to asymptotic value of g modes, $\beta_{k,l=1} = 0.5$, $\beta_{k,l=2} = 0.833$, and $\beta_{k,l=3} = 0.917$.

For the three identified $l = 1$ modes f_{12} , f_{34} , and f_{43} , their corresponding $\beta_{k,l}$ of these candidate modes are listed in Table 4. In Table 4, rotational parameters $\beta_{k,l}$ of observed frequencies are asymptotic values of g modes based on Equation (1). It can be found in Table 4 that theoretical values of $\beta_{k,l}$ for Model 1, 2, 3, and 7 significantly deviate from those asymptotic values of g modes. We therefore exclude these four models from our considerations. The physical parameters of CoRoT 102749568 are obtained based on Model 4, 5,

and 6. These parameters are listed in Table 5. In our work, we select the theoretical model (Model 4) with minimum value of $\chi^2 = 0.016$ as the optimal model. Its theoretical evolutionary track corresponds to the curve in Figure 1.

Theoretical pulsation frequencies of the optimal model are listed in Table 6, in which n_p is the amount of radial nodes in the propagation of p modes and n_g the amount of radial nodes in the propagation of g modes. We notice in Table 6 that most of the pulsation modes are gravity and mixed modes. Figure 3 shows the plot of $\beta_{k,l}$ to theoretical pulsation frequencies for the optimal model. We can find in Figure 3 that most of $\beta_{k,l}$ are in good agreement with the asymptotic value of g modes. These pulsation modes possess more pronounced g-mode features. Besides, there are several pulsation modes, whose $\beta_{k,l}$ obviously deviate from the asymptotic values of g modes. They have more pronounced p-mode features.

Comparisons of results of pulsation frequencies in Table 2 are listed in Table 7. The $m \neq 0$ pulsation frequencies in columns denoted with ν^{theo} are derived from $m = 0$ modes according to Equation (1). The filled circles in Figure 3 correspond to $m = 0$ components of the multiplets in Table 7. It can be noticed in Table 7 that $m = 0$ components in Multiplet 1, 2, 3, 5, 9, 10, 14, and 18 are observed, while $m = 0$ components in Multiplet 4, 6, 7, 8, 11, 12, 13, 15, 16, 17, 19, 20, and 21 are absent. In Figure 3, we notice that $\beta_{k,l}$ of $m = 0$ components in Multiplet 1, 2, 3, 5, 9, 10, 14, and 18 agree well with the asymptotic value of g modes. For Multiplet 4, 6, 7, 8, 11, 12, 15, 16, 17, 19, 20, and 21, $\beta_{k,l}$ of their corresponding $m = 0$ components are also in accordance with Equation (1). Moreover, we find that $\beta_{k,l}$ of corresponding $m = 0$ components in Multiplet 13 are slightly larger than the asymptotic value from Equation (1). These results also proves that our approach of mode identification based on the rotational splitting of g modes is self-consistent.

Finally, we try to do mode identification for the three isolated pulsation frequencies based on the optimal model, and list them in Table 8. We notice in Table 8 that there are two possible model counterparts for f_4 , i.e., $(1, 0, -51, -1)$ $76.394 \mu\text{Hz}$ and $(2, 0, -117, +2)$ $76.303 \mu\text{Hz}$. For f_{40} , $(2, 3, -35, +2)$ $190.803 \mu\text{Hz}$ may be possible model counterpart. According to the analyses in Section 2, the spherical harmonic degree of f_{48} allows of two possibilities, i.e., $l = 2$ and $l = 3$. When identifying f_{48} and f_{51} as being two $l = 2$ modes, their possible model counterparts are listed in Table 7. If f_{48} and f_{52} are identified as being two $l = 3$ modes, there are no suitable model counterparts for them.

4. DISCUSSIONS

When doing model fittings, we use four identified pulsation modes including the radial first overtone f_{13} and three $l = 1$ modes (f_{12} , f_{34} , and f_{43}). Figure 4 shows the propagation diagram of the optimal model. Based on the default parameters, we adopt the position where the hydrogen fraction $X_{cb} = 0.01$ as the boundary of the helium core. The outer zone is the stellar envelope, and the inner zone is the helium core. The vertical curves in Figures 4 and 5 indicate the boundary of the helium core. Figure 5 shows the scaled eigenfunctions of the radial first overtone and the three $l = 1$ nonradial pulsation modes. It can be seen clearly in Figure 5 that the radial first overtone mainly propagates in the stellar envelope, and therefore mainly provide constraints on the stellar envelope. For the three nonradial pulsation modes, Figure 5 shows that they behave g-mode features in the helium core and p-mode features in the stellar envelope. Then the three nonradial pul-

sation modes mainly provide constraints on the helium core.

Following Chen et al. (2016), we introduce two asteroseismic parameters, i.e., the acoustic radius τ_0 and the period separation Π_0 . The acoustic radius τ_0 is a significant physical parameter in the asteroseismic study. The acoustic radius τ_0 carries information on the stellar envelope (e.g., Ballot et al. 2004; Miglio et al. 2010; Chen et al. 2016). The acoustic radius τ_0 is defined as (Aerts et al. 2010)

$$\tau_0 = \int_0^R \frac{dr}{c_s}, \quad (5)$$

in which R is the stellar radius and c_s the adiabatic sound speed. According to Equation (5), the value of acoustic radius τ_0 is mainly dominated by the profile of c_s inside the stellar envelope.

According to the theory of stellar oscillations, g-mode oscillations are gravity waves. They mainly propagate inside the helium core. Their properties can be characterized by Π_0 , which is defined as

$$\Pi_0 = 2\pi^2 \left(\int_0^R \frac{N}{r} dr \right)^{-1} \quad (6)$$

(Unno et al. 1979; Tassoul 1980; Aerts et al. 2010), where N is the Brunt-Väisälä frequency. According to Equation (6), Π_0 is mainly dominated by the profile of Brunt-Väisälä frequency N inside the helium core.

To fit the four pulsation modes (f_{12} , f_{13} , f_{34} , and f_{43}), both the helium core and the stellar envelope of the theoretical model need to be matched to the actual structure of CoRoT 102749568. It can be found in Table 3 that τ_0 and Π_0 of the three preferred models (Model 4, 5, and 6) are very close. This is because they are nearly alike in structure. Thus the size of the helium core of CoRoT 102749568 is determined to be $M_{\text{He}} = 0.148 \pm 0.003 M_{\odot}$ and $R_{\text{He}} = 0.0581 \pm 0.0007 R_{\odot}$. The errors are estimated on basis of the deviations of the helium cores of Model 5 and 6 from that of Model 4.

According to Equation (1), the rotational period P_{rot} of the δ Scuti star CoRoT 102749568 is determined to be $P_{\text{rot}} = 1.34_{-0.05}^{+0.04}$ days. Meanwhile, we find in Table 5 that the theoretical radius R of CoRoT 102749568 is $2.916 \pm 0.039 R_{\odot}$. According to $v_{\text{rot}} = 2\pi R/P_{\text{rot}}$, the rotational velocity at the equator is then deduced to be $v_{\text{rot}} = 109.8_{-4.6}^{+6.4}$ km s $^{-1}$, which is in agreement with the value of $v \sin i = 115 \pm 20$ km s $^{-1}$ (Paparó et al. 2013).

It should be noticed that Equation (1) only contains the first-order effect of rotation $C_1 m/P_{\text{rot}}$, in which $C_1 = 1 - \frac{1}{L^2}$. The second-order effect of rotation is derived by Dziembowski & Goode (1992) as being $\frac{m^2 C_2}{P_{\text{rot}}^2 \nu_{k,l,0}}$, the coefficient $C_2 = \frac{4L^2(2L^2-3)-9}{2L^4(4L^2-3)}$. The ratio of the second-order effect and the first-order effect is then deduced to be $\phi_l = \frac{C_2}{C_1} \frac{m}{P_{\text{rot}} \nu_{k,l,0}}$. Assuming $\nu_{k,l,0} = 100 \mu\text{Hz}$, the absolute value of $\phi_{l=1}$ is estimated to be 0.0043, $\phi_{l=2}$ to be 0.0141 $|m|$, and $\phi_{l=3}$ to be 0.0073 $|m|$. For pulsation modes with $l = 1$, the second-order effect is 0.43% that of the first-order. For pulsation modes with $l = 2$ and $l = 3$, the ratios $\phi_{l=2}$ and $\phi_{l=3}$ are in direct proportion to the azimuthal number m . The second-order effect is 2.82% that of the first-order for modes with $l = 2$ and $|m| = 2$. The second-order effect is 2.19% that of the first-order for modes with $l = 3$ and $|m| = 3$. In brief, the second-order effect of stellar rotation is much less than that

of the first-order. Hence the second-order effect of rotation is not considered in our work.

Finally, our model fitting results show that a slight increase in the convective core size is essential to explain these multiplets. There are two different ways to increase the convective core size, i.e., convective core overshooting (Herwig 2000; Li & Yang 2007; Zhang 2013) and rotation (Eggenberger et al. 2010; Girardi et al. 2011). Maeder & Meynet (2000) and Yang et al. (2013) found that the effects of rotation on stellar structure and evolution depend on the masses of stellar models. Moreover, Yang et al. (2013) noticed that $2.05 M_{\odot}$ is a critical mass. Rotation results in an increase in the convective core size for stars with $M > 2.05 M_{\odot}$. The effect is similar to that of the convective core overshooting. However for stars with $M < 2.05 M_{\odot}$, rotation leads to a decrease in the convective core size. The optimal model in our work corresponds to a star with $M = 1.54 M_{\odot}$, $Z = 0.006$, $f_{\text{ov}} = 0.004$. According to the analyses of Yang et al. (2013), rotation will result in a slight decrease in the convective core size. If the effects of rotation are included in theoretical evolutionary models, a larger convective core overshooting may be indispensable.

5. SUMMARY

In this work, we carry out asteroseismic analyses and numerical calculations for the δ Scuti star CoRoT 102749568. The main results are concluded as follows:

1. We identify twenty-one sets of multiplets using the regularities in rotational splittings, including four sets of multiplets with $l = 1$, nine sets of multiplets with $l = 2$, and eight sets of multiplets with $l = 3$. In particular, there are three complete triplets, i.e., (f_{10} , f_{12} , f_{14}), (f_{31} , f_{34} , f_{35}), and (f_{41} , f_{43} , f_{44}). The rotational period P_{rot} is estimated to be $1.34_{-0.05}^{+0.04}$ days according to the frequency differences in these multiplets.

2. Based on our model calculations, the δ Scuti star CoRoT 102749568 is in post-main-sequence evolution stage. The stellar parameters of the δ Scuti star CoRoT 102749568 are determined to be $M = 1.54 \pm 0.03 M_{\odot}$, $Z = 0.006$, $f_{\text{ov}} = 0.004 \pm 0.002$, $\log g = 3.696 \pm 0.003$, $T_{\text{eff}} = 6886 \pm 70$ K, $R = 2.916 \pm 0.039 R_{\odot}$, and $L = 17.12 \pm 1.13 L_{\odot}$.

3. Based on our optimal model, we notice that most of the oscillation frequencies are mixed modes. The radial first overtone f_{13} mainly provides constraints on the stellar envelope. The three nonradial pulsation modes f_{12} , f_{34} , and f_{43} possess more pronounced g-mode features, which mainly provide constraints on the helium core. The property of the stellar envelope is characterized by the acoustic radius τ_0 , and the property of the helium core is characterized by the period separation Π_0 . Finally, the size of the helium core of CoRoT 102749568 is determined to be $M_{\text{He}} = 0.148 \pm 0.003 M_{\odot}$ and $R_{\text{He}} = 0.0581 \pm 0.0007 R_{\odot}$.

This work is funded by the NSFC of China (Grant No. 11333006, 11521303, 11503079, and 11563001) and by the foundation of Chinese Academy of Sciences (Grant No. XDB09010202). The authors gratefully acknowledge the computing time granted by the Yunnan Observatories, and provided on the facilities at the Yunnan Observatories Supercomputing Platform. The authors are sincerely grateful to an anonymous referee for instructive advice and productive suggestions. The authors are also very grateful to the suggestions from Q.-S. Zhang, T. Wu, and J. Su.

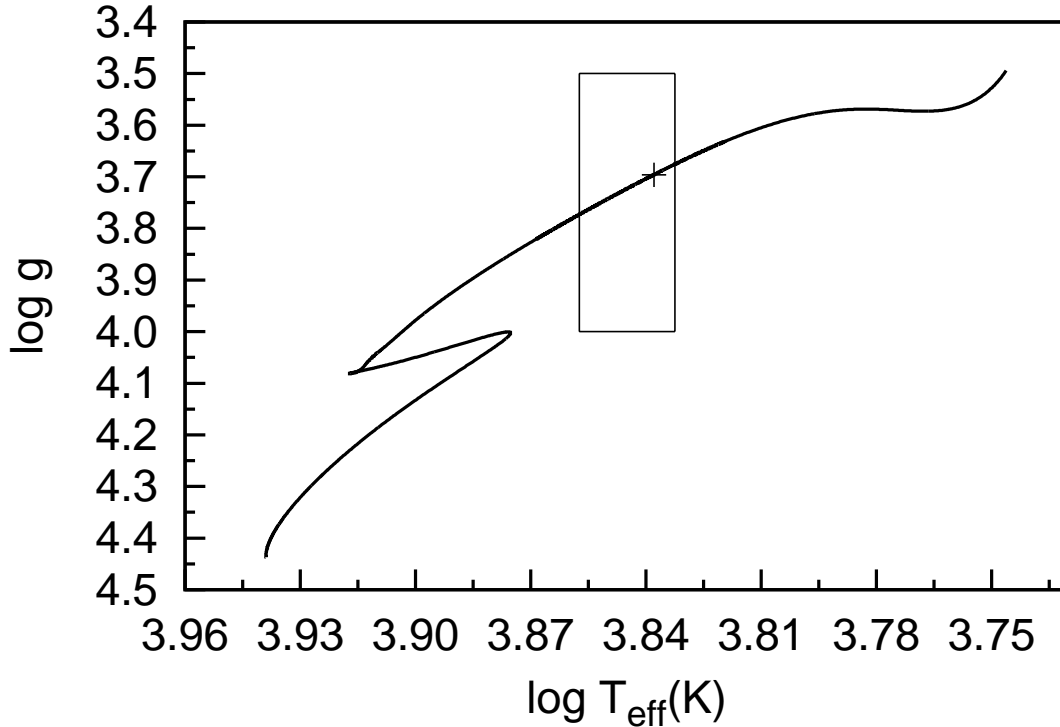


FIG. 1.— Evolutionary track of $M=1.54 M_{\odot}$, $Z=0.006$, $f_{ov}=0.004$. The rectangle corresponds to the error box of the observed parameters, $3.5 < \log g < 4.0$ and $6800 \text{ K} < T_{\text{eff}} < 7200 \text{ K}$. The cross marks the location of the optimal model (Model 4).

REFERENCES

- Aerts, C., Christensen-Dalsgaard, J., & Kurtz, D. W. 2010, *Asteroseismology*, Astronomy and Astrophysics Library. ISBN 978-1-4020-5178-4. Springer Science+Business Media B.V., 2010
- Aizenman, M., Smeyers, P., & Weigert, A. 1977, *A&A*, 58, 41
- Baglin, A., Auvergne, M., Barge, P., et al. 2006, *The CoRoT Mission Pre-Launch Status - Stellar Seismology and Planet Finding*, 1306, 33
- Ballot, J., Turck-Chièze, S., & García, R. A. 2004, *A&A*, 423, 1051
- Breger, M., Balona, L., Lenz, P., et al. 2011, *MNRAS*, 414, 1721
- Brickhill, A. J. 1975, *MNRAS*, 170, 405
- Böhm-Vitense, E. 1958, *Z. Astrophys.*, 46, 108
- Borucki, W. J., Koch, D., Basri, G., et al. 2010, *Science*, 327, 977
- Chen, X. H., Li, Y., Lai, X. J., & Wu, T. 2016, *A&A*, 593, A69
- Christensen-Dalsgaard, J. 2003, *Lecture notes on Stellar Oscillations*, 5th edn (Institut for Fysik og Astronomi, Aarhus Universitet)
- Christensen-Dalsgaard, J. 2008, *Ap&SS*, 316, 113
- Dotter, A., Chaboyer, B., Jevremović, D., et al. 2008, *ApJS*, 178, 89-101
- Dziembowski, W. A., & Goode, P. R. 1992, *ApJ*, 394, 670
- Eggenberger, P., Miglio, A., Montalbán, J., et al. 2010, *A&A*, 509, A72
- Freytag, B., Ludwig, H.-G., & Steffen, M. 1996, *A&A*, 313, 497
- García Hernández, A., Moya, A., Michel, E., et al. 2009, *A&A*, 506, 79
- García Hernández, A., Moya, A., Michel, E., et al. 2013, *A&A*, 559, A63
- Girardi, L., Eggenberger, P., & Miglio, A. 2011, *MNRAS*, 412, L103
- Grevesse, N., & Sauval, A. J. 1998, *Space Sci. Rev.*, 85, 161
- Guenther, E. W., Gandolfi, D., Sebastian, D., et al. 2012, *A&A*, 543, A125
- Herwig, F. 2000, *A&A*, 360, 952
- Kurucz, R. L. 1979, *ApJS*, 40, 1
- Li, Y., & Yang, J. Y. 2007, *MNRAS*, 375, 388
- Lignières, F., Rieutord, M., & Reese, D. 2006, *A&A*, 455, 607
- Maeder, A., & Meynet, G. 2000, *ARA&A*, 38, 143
- Mantegazza, L., Poretti, E., Michel, E., et al. 2012, *A&A*, 542, A24
- Miglio, A., Montalbán, J., Carrier, F., et al. 2010, *A&A*, 520, L6
- Paparo, M., Bognár, Z., Benkő, J. M., et al. 2013, *A&A*, 557, A27
- Paparo, M., Benkő, J. M., Hareter, M., & Guzik, J. A. 2016, *ApJ*, 822, 100
- Paxton, B., Bildsten, L., Dotter, A., et al. 2011, *ApJS*, 192, 3
- Paxton, B., Cantiello, M., Arras, P., et al. 2013, *ApJS*, 208, 4
- Poretti, E., Michel, E., Garrido, R., et al. 2009, *A&A*, 506, 85
- Straizys, V., & Kuriliene, G. 1981, *Ap&SS*, 80, 353
- Tassoul, M. 1980, *ApJS*, 43, 469
- Thompson, B., Frinchaboy, P., Kinemuchi, K., Sarajedini, A., & Cohen, R. 2014, *AJ*, 148, 85
- Tian, Z., Bi, S., Bedding, T. R., & Yang, W. 2015, *A&A*, 580, A44
- Unno, W., Osaki, Y., Ando, H., & Shibahashi, H. 1979, *Nonradial oscillations of stars* (University of Tokyo Press)
- Walker, G., Matthews, J., Kuschnig, R., et al. 2003, *PASP*, 115, 1023
- Winget, D. E., Nather, R. E., Clemens, J. C., et al. 1991, *ApJ*, 378, 326
- Yang, W.-M., Bi, S.-L., & Meng, X.-C. 2013, *Research in Astronomy and Astrophysics*, 13, 579-592
- Zhang, Q. S. 2013, *ApJS*, 205, 18
- Zwintz, K., Lenz, P., Breger, M., et al. 2011, *A&A*, 533, A133

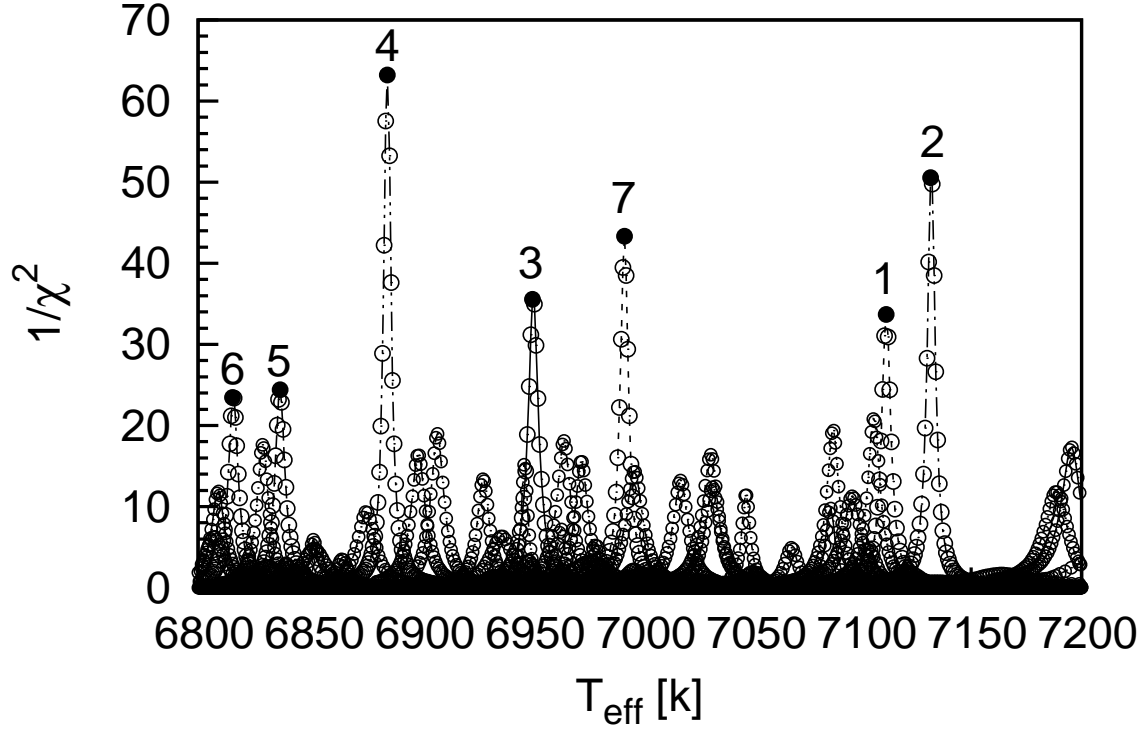


FIG. 2.— Plot of $1/\chi^2$ to the effective temperature T_{eff} of all theoretical models. The filled circles indicate the candidate models in Table 3.

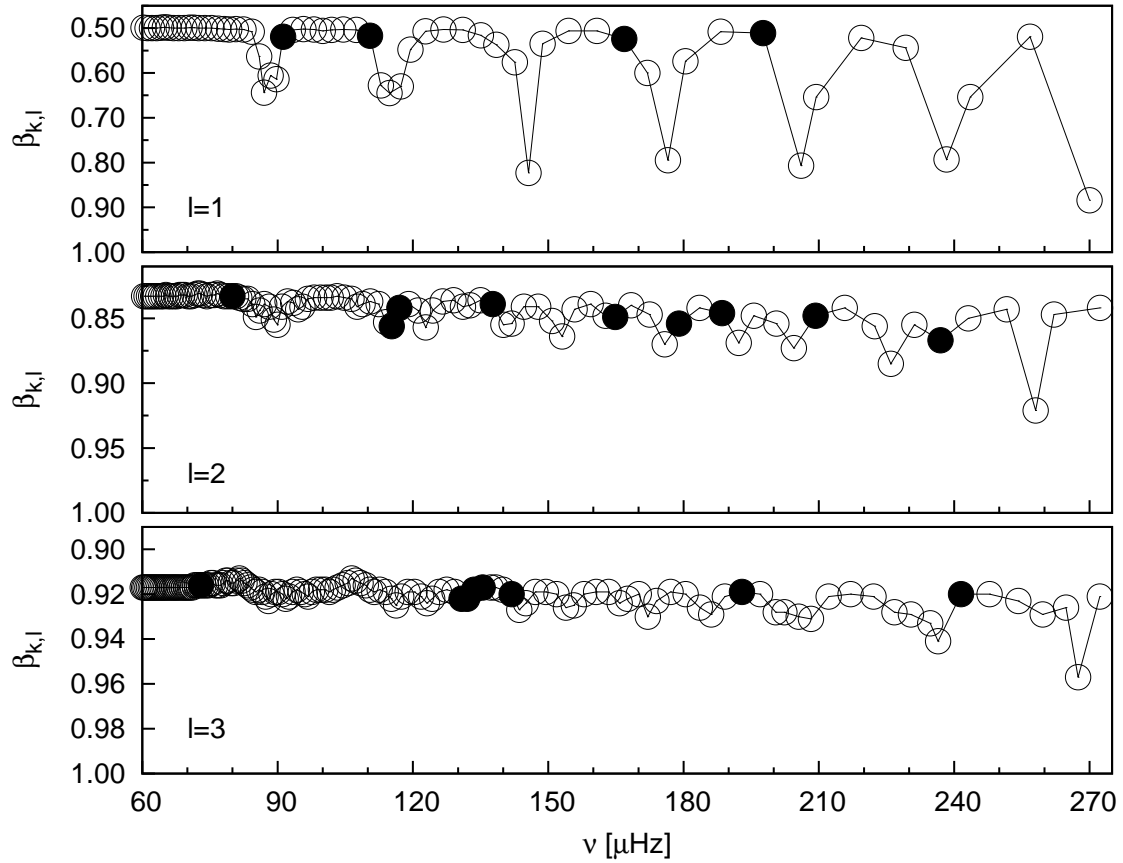


FIG. 3.— Plot of $\beta_{k,l}$ versus theoretically calculated frequency ν of the optimal model. The filled circles correspond to $m = 0$ components of the multiplets in Table 7.

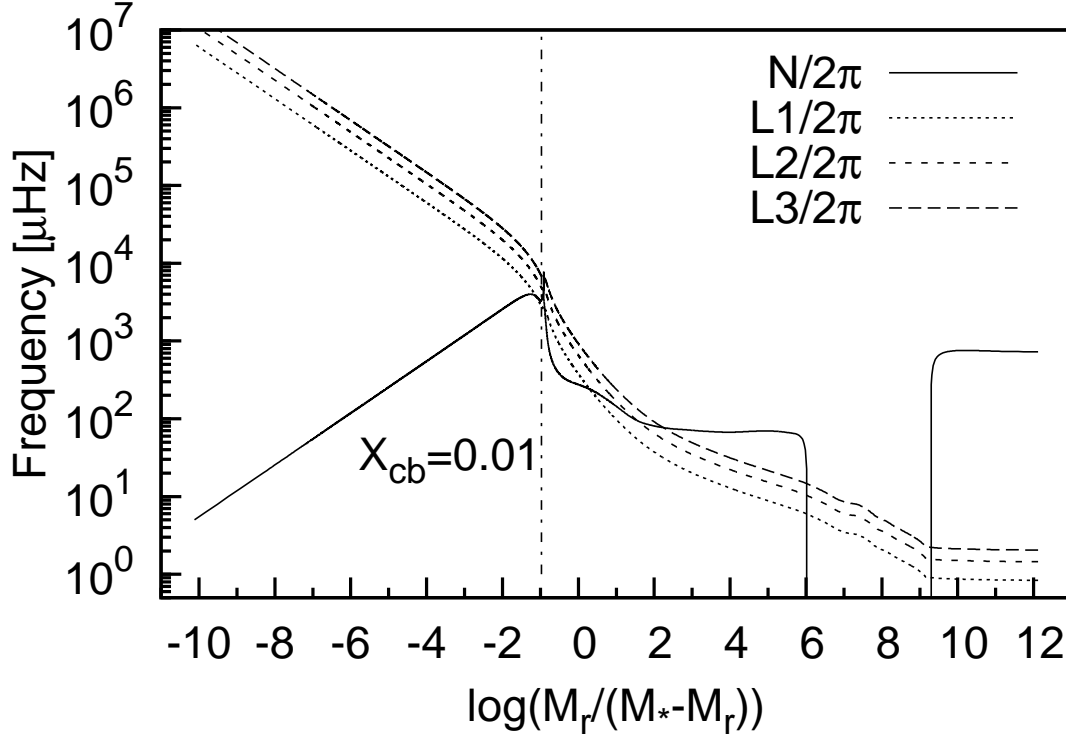


FIG. 4.— N is Brunt–Väisälä frequency and L_l ($l = 1, 2, 3$) are Lamb frequency. M_* is the stellar mass. The vertical line indicates the boundary of the helium core.

TABLE 1

THE 52 INDEPENDENT FREQUENCIES OF CoRoT 102749568 OBTAINED BY PAPAŘÓ ET AL. (2013). THE COLUMNS NAMED BY ID ARE THE SERIAL NUMBER OF OBSERVED FREQUENCIES. FREQ. INDICATES THE OBSERVED FREQUENCY IN UNIT OF μHz . AMPL. INDICATES THE AMPLITUDE IN UNIT OF MMAG.

ID	Freq. (μHz)	Ampl. (mmag)	ID	Freq. (μHz)	Ampl. (mmag)
f_1	64.936	0.16	f_{27}	141.765	1.01
f_2	65.541	0.18	f_{28}	144.934	0.27
f_3	72.978	0.18	f_{29}	155.380	0.23
f_4	76.363	0.25	f_{30}	158.977	0.27
f_5	87.275	0.25	f_{31}	162.625	0.29
f_6	96.149	1.75	f_{32}	164.262	0.17
f_7	96.938	0.75	f_{33}	164.855	0.73
f_8	100.779	0.26	f_{34}	167.007	0.14
f_9	102.072	0.14	f_{35}	171.485	0.23
f_{10}	106.152	0.39	f_{36}	171.638	0.23
f_{11}	108.372	0.43	f_{37}	172.243	0.22
f_{12}	110.637	1.44	f_{38}	176.285	0.15
f_{13}	112.291	10.51	f_{39}	189.056	0.16
f_{14}	115.036	4.77	f_{40}	190.612	0.14
f_{15}	115.706	0.41	f_{41}	192.909	0.16
f_{16}	115.872	0.22	f_{42}	194.179	0.68
f_{17}	117.666	0.23	f_{43}	197.503	0.15
f_{18}	122.559	0.27	f_{44}	201.898	0.20
f_{19}	122.769	0.88	f_{45}	203.652	0.60
f_{20}	123.812	0.17	f_{46}	209.708	0.14
f_{21}	124.571	0.19	f_{47}	216.758	0.17
f_{22}	125.296	0.92	f_{48}	222.367	0.18
f_{23}	132.028	0.19	f_{49}	233.083	0.24
f_{24}	133.453	1.21	f_{50}	249.725	0.15
f_{25}	134.071	0.19	f_{51}	252.079	0.14
f_{26}	134.762	3.66	f_{52}	262.964	0.16

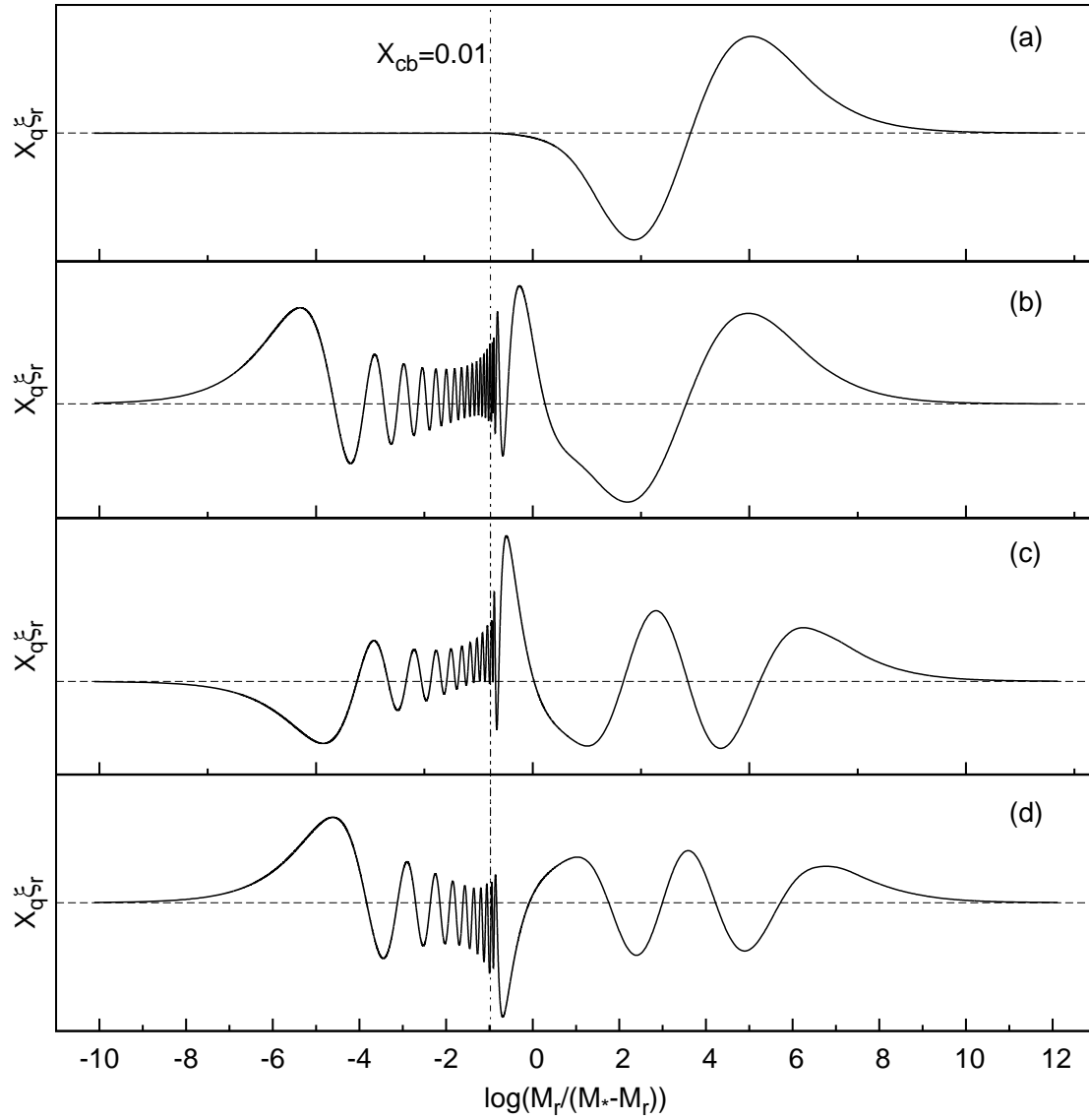


FIG. 5.— Scaled eigenfunctions of the radial first overtone f_{13} and the three nonradial modes f_{12} , f_{34} , and f_{43} . $X_q = \sqrt{q(1-q)}$ and $q = M_r/M_*$. Panel (a) is for the radial first overtone $112.212 \mu\text{Hz}$ ($l = 0, n_p = 1, n_g = 0$). Panel (b) is for the mode $110.476 \mu\text{Hz}$ ($l = 1, n_p = 1, n_g = -37$). Panel (c) is for the mode $166.873 \mu\text{Hz}$ ($l = 1, n_p = 3, n_g = -24$). Panel (d) is for the mode $197.617 \mu\text{Hz}$ ($l = 1, n_p = 4, n_g = -20$). Vertical line indicates the boundary of the helium core.

TABLE 2
POSSIBLE MULTIPLETS DUE TO STELLAR ROTATION. $\delta\nu$ = FREQUENCY DIFFERENCE IN μHz

Multiplet	ID	Freq. (μHz)	$\delta\nu$ (μHz)	l	m	Multiplet	ID	Freq. (μHz)	$\delta\nu$ (μHz)	l	m
1	f_{10}	106.152	4.485	1	-1	11	f_{18}	122.559	22.375	2	(-2, -1)
	f_{12}	110.637		1	0		f_{28}	144.934		2	(+1, +2)
	f_{14}	115.036	4.399	1	+1	12	f_{42}	194.179	22.579	2	(-2, -1)
2	f_{31}	162.625	4.382	1	-1		f_{47}	216.758		2	(+1, +2)
	f_{34}	167.007		1	0	13	f_{48}	222.367	29.712	2	-2
	f_{35}	171.485	4.478	1	+1		f_{51}	252.079		2	+2
3	f_{41}	192.909	4.594	1	-1	14	f_{22}	125.296	8.157	3	(-3, -2, -1, 0, +1)
	f_{43}	197.503		1	0		f_{24}	133.453		3	(-2, -1, 0, +1, +2)
	f_{44}	201.898	4.395	1	+1	f_{27}	141.765	3	(-1, 0, +1, +2, +3)		
4	f_5	87.275	8.874	1	-1	15	f_{15}	115.706	8.106	3	(-3, -2, -1, 0, +1, +2)
	f_6	96.149		1	+1		f_{20}	123.812		3	(-2, -1, 0, +1, +2, +3)
5	f_8	100.779	7.593	2	(-2, -1, 0)	16	f_{17}	117.666	16.405	3	(-3, -2, -1, 0, +1)
	f_{11}	108.372		2	(-1, 0, +1)		f_{25}	134.071		3	(-1, 0, +1, +2, +3)
	f_{16}	115.872	7.500	2	(0, +1, +2)	17	f_{49}	233.083	16.642	3	(-3, -2, -1, 0, +1)
6	f_9	102.072	22.499	2	-2		f_{50}	249.725		3	(-1, 0, +1, +2, +3)
	f_{21}	124.571		2	+1	18	f_{26}	134.762	24.215	3	(-3, -2, -1, 0)
	f_{23}	132.028	7.457	2	+2		f_{30}	158.977		3	(0, +1, +2, +3)
7	f_2	65.541	7.437	2	(-2, -1, 0, +1)	19	f_1	64.936	32.002	3	(-3, -2, -1)
	f_3	72.978		2	(-1, 0, +1, +2)		f_7	96.938		3	(+1, +2, +3)
8	f_{32}	164.262	7.376	2	(-2, -1, 0, +1)	20	f_{19}	122.769	32.611	3	(-3, -2, -1)
	f_{36}	171.638		2	(-1, 0, +1, +2)		f_{29}	155.380		3	(+1, +2, +3)
9	f_{33}	164.855	7.388	2	(-2, -1, 0, +1)	21	f_{38}	176.285	33.423	3	(-3, -2, -1)
	f_{37}	172.243		2	(-1, 0, +1, +2)		f_{46}	209.708		3	(+1, +2, +3)
10	f_{39}	189.056	14.596	2	(-2, -1, 0)						
	f_{45}	203.652		2	(0, +1, +2)						

TABLE 3
CANDIDATE MODELS WITH $\chi^2 < 0.05$ OF FOUR OBSERVED FREQUENCIES FOR THE δ SCUTI STAR CORoT 102749568.

Model	Z	M [M_{\odot}]	f_{ov}	T_{eff} [K]	$\log g$ [dex]	R [R_{\odot}]	L [L_{\odot}]	τ_0 [h]	Π_0 [s]	χ^2
1	0.010	1.74	0	7111	3.706	3.065	21.52	4.21	431.1	0.030
2	0.010	1.75	0	7132	3.704	3.080	21.99	4.23	430.7	0.020
3	0.006	1.57	0.001	6951	3.693	2.953	18.24	4.14	330.0	0.028
4	0.006	1.54	0.004	6886	3.696	2.916	17.12	4.08	331.8	0.016
5	0.006	1.52	0.005	6837	3.698	2.889	16.34	4.03	331.5	0.041
6	0.006	1.51	0.006	6816	3.699	2.877	15.99	4.01	331.8	0.043
7	0.007	1.59	0.013	6993	3.695	2.965	18.84	4.16	427.7	0.023

TABLE 4
THEORETICAL ROTATIONAL PARAMETERS OF THE THREE NONRADIAL PULSATION MODES (f_{12} , f_{34} , AND f_{43}) FOR THE CANDIDATE MODELS IN TABLE 3. THE ROTATIONAL PARAMETERS $\beta_{k,l}$ OF OBSERVED FREQUENCIES INSIDE BRACKETS ARE THE ASYMPTOTIC VALUE OF G MODES ACCORDING TO EQUATION (1).

Model	$f_{12}(\beta_{k,l})$ (μHz)	$f_{34}(\beta_{k,l})$ (μHz)	$f_{43}(\beta_{k,l})$ (μHz)
obs	110.637(0.5)	167.007(0.5)	197.503(0.5)
1	110.618(0.519)	166.977(0.528)	197.704(0.541)
2	110.622(0.528)	166.843(0.535)	197.606(0.553)
3	110.411(0.538)	167.118(0.514)	197.421(0.537)
4	110.476(0.517)	166.873(0.524)	197.617(0.511)
5	110.332(0.511)	167.215(0.513)	197.401(0.508)
6	110.440(0.523)	166.798(0.516)	197.773(0.507)
7	110.753(0.573)	167.170(0.570)	197.499(0.522)

TABLE 5
FUNDAMENTAL PARAMETERS OF THE δ SCUTI STAR CORoT 102749568.

Parameter	Values
M/M_{\odot}	1.54 ± 0.03
Z	0.006
f_{ov}	0.004 ± 0.002
$T_{\text{eff}} [K]$	6886 ± 70
$\log g$	3.696 ± 0.003
R/R_{\odot}	2.916 ± 0.039
L/L_{\odot}	17.12 ± 1.13
M_{He}/M_{\odot}	0.148 ± 0.003
R_{He}/R_{\odot}	0.0581 ± 0.0007

TABLE 6

THEORETICALLY CALCULATED FREQUENCIES OF THE OPTIMAL MODEL. ν^{theo} DENOTES CALCULATED FREQUENCY IN μHz . n_p IS THE AMOUNT OF RADIAL NODES IN PROPAGATION CAVITY OF P MODES. n_g IS THE AMOUNT OF RADIAL NODES IN PROPAGATION CAVITY OF G MODES. $\beta_{k,l}$ IS ONE ROTATIONAL PARAMETER MEASURING THE SIZE OF ROTATIONAL SPLITTING.

$\nu^{\text{theo}}(l, n_p, n_g)$ (μHz)	$\beta_{k,l}$	$\nu^{\text{theo}}(l, n_p, n_g)$ (μHz)	$\beta_{k,l}$	$\nu^{\text{theo}}(l, n_p, n_g)$ (μHz)	$\beta_{k,l}$	$\nu^{\text{theo}}(l, n_p, n_g)$ (μHz)	$\beta_{k,l}$	$\nu^{\text{theo}}(l, n_p, n_g)$ (μHz)	$\beta_{k,l}$
86.446(0, 0, 0)		60.956(2, 0, -119)	0.833	121.149(2, 1, -58)	0.844	68.292(3, 0, -150)	0.917	112.635(3, 1, -89)	0.918
112.212(0, 1, 0)		61.482(2, 0, -118)	0.833	122.819(2, 2, -58)	0.857	68.772(3, 0, -149)	0.917	113.962(3, 1, -88)	0.919
140.555(0, 2, 0)		61.955(2, 0, -117)	0.833	124.380(2, 2, -57)	0.844	69.238(3, 0, -148)	0.917	115.230(3, 1, -87)	0.922
170.701(0, 3, 0)		62.414(2, 0, -116)	0.833	126.576(2, 2, -56)	0.837	69.665(3, 0, -147)	0.917	116.273(3, 1, -86)	0.925
201.509(0, 4, 0)		62.948(2, 0, -115)	0.833	128.974(2, 2, -55)	0.836	70.089(3, 0, -146)	0.917	117.415(3, 1, -85)	0.921
232.369(0, 5, 0)		63.532(2, 0, -114)	0.833	131.076(2, 2, -54)	0.841	70.565(3, 0, -145)	0.917	118.825(3, 1, -84)	0.919
263.224(0, 6, 0)		64.130(2, 0, -113)	0.833	132.641(2, 2, -53)	0.840	71.076(3, 0, -144)	0.917	120.332(3, 1, -83)	0.919
		64.703(2, 0, -112)	0.833	134.982(2, 2, -52)	0.836	71.596(3, 0, -143)	0.916	121.821(3, 1, -82)	0.921
70.483(1, 0, -59)	0.499	65.208(2, 0, -111)	0.832	137.679(2, 2, -51)	0.839	72.092(3, 0, -142)	0.916	123.096(3, 1, -81)	0.924
71.418(1, 0, -58)	0.499	65.726(2, 0, -110)	0.833	140.046(2, 2, -50)	0.855	72.543(3, 0, -141)	0.916	124.285(3, 1, -80)	0.922
72.506(1, 0, -57)	0.500	66.333(2, 0, -109)	0.833	141.883(2, 2, -49)	0.854	73.009(3, 0, -140)	0.916	125.794(3, 1, -79)	0.919
73.862(1, 0, -56)	0.500	66.987(2, 0, -108)	0.833	144.601(2, 2, -48)	0.841	73.536(3, 0, -139)	0.916	127.481(3, 2, -79)	0.918
75.327(1, 0, -55)	0.500	67.649(2, 0, -107)	0.833	147.760(2, 2, -47)	0.841	74.095(3, 0, -138)	0.916	129.203(3, 2, -78)	0.919
76.814(1, 0, -54)	0.501	68.269(2, 0, -106)	0.832	150.828(2, 2, -46)	0.852	74.655(3, 0, -137)	0.916	130.767(3, 2, -77)	0.922
78.139(1, 0, -53)	0.502	68.812(2, 0, -105)	0.832	153.094(2, 2, -45)	0.864	75.177(3, 0, -136)	0.915	132.033(3, 2, -76)	0.922
79.258(1, 0, -52)	0.503	69.408(2, 0, -104)	0.832	155.838(2, 3, -45)	0.843	75.656(3, 0, -135)	0.915	133.602(3, 2, -75)	0.918
80.717(1, 0, -51)	0.502	70.101(2, 0, -103)	0.833	159.389(2, 3, -44)	0.839	76.178(3, 0, -134)	0.916	135.456(3, 2, -74)	0.917
82.436(1, 0, -50)	0.503	70.836(2, 0, -102)	0.833	162.691(2, 3, -43)	0.848	76.763(3, 0, -133)	0.916	137.243(3, 2, -73)	0.917
84.244(1, 0, -49)	0.508	71.568(2, 0, -101)	0.832	164.831(2, 3, -42)	0.849	77.372(3, 0, -132)	0.916	138.534(3, 2, -72)	0.917
85.900(1, 0, -48)	0.563	72.226(2, 0, -100)	0.831	168.348(2, 3, -41)	0.840	77.966(3, 0, -131)	0.915	139.917(3, 2, -71)	0.918
86.984(1, 0, -47)	0.644	72.820(2, 0, -99)	0.831	172.456(2, 3, -40)	0.847	78.498(3, 0, -130)	0.914	141.887(3, 2, -70)	0.920
88.472(1, 0, -46)	0.606	73.523(2, 0, -98)	0.832	175.818(2, 3, -39)	0.870	79.017(3, 0, -129)	0.914	143.568(3, 2, -69)	0.927
89.761(1, 1, -46)	0.614	74.320(2, 0, -97)	0.833	178.990(2, 3, -38)	0.854	79.615(3, 0, -128)	0.915	145.066(3, 2, -68)	0.924
91.237(1, 1, -45)	0.519	75.147(2, 0, -96)	0.832	183.554(2, 3, -37)	0.842	80.264(3, 0, -127)	0.915	147.132(3, 2, -67)	0.919
93.371(1, 1, -44)	0.504	75.942(2, 0, -95)	0.832	188.534(2, 4, -37)	0.846	80.910(3, 0, -126)	0.914	149.459(3, 2, -66)	0.919
95.705(1, 1, -43)	0.502	76.619(2, 0, -94)	0.831	192.235(2, 4, -36)	0.869	81.486(3, 0, -125)	0.913	151.823(3, 2, -65)	0.920
98.039(1, 1, -42)	0.503	77.309(2, 0, -93)	0.832	195.553(2, 4, -35)	0.848	82.016(3, 0, -124)	0.914	153.906(3, 2, -64)	0.926
100.008(1, 1, -41)	0.506	78.153(2, 0, -92)	0.833	200.574(2, 4, -34)	0.854	82.643(3, 0, -123)	0.915	155.655(3, 2, -63)	0.925
101.955(1, 1, -40)	0.504	79.068(2, 0, -91)	0.833	204.466(2, 4, -33)	0.873	83.332(3, 0, -122)	0.916	157.949(3, 2, -62)	0.920
104.540(1, 1, -39)	0.503	79.981(2, 0, -90)	0.833	209.244(2, 4, -32)	0.848	84.004(3, 0, -121)	0.917	160.619(3, 3, -62)	0.919
107.462(1, 1, -38)	0.504	80.774(2, 0, -89)	0.833	215.729(2, 4, -31)	0.842	84.576(3, 0, -120)	0.918	163.381(3, 3, -61)	0.919
110.476(1, 1, -37)	0.517	81.481(2, 0, -88)	0.834	222.360(2, 5, -31)	0.856	85.165(3, 0, -119)	0.919	165.825(3, 3, -60)	0.924
112.907(1, 1, -36)	0.628	82.374(2, 0, -87)	0.835	225.926(2, 5, -30)	0.885	85.875(3, 0, -118)	0.918	167.604(3, 3, -59)	0.922
114.805(1, 1, -35)	0.645	83.381(2, 0, -86)	0.835	231.158(2, 5, -29)	0.855	86.630(3, 0, -117)	0.919	170.052(3, 3, -58)	0.920
117.293(1, 2, -35)	0.630	84.384(2, 0, -85)	0.839	236.938(2, 5, -28)	0.867	87.352(3, 0, -116)	0.921	172.081(3, 3, -57)	0.930
119.439(1, 2, -34)	0.548	85.209(2, 0, -84)	0.849	243.129(2, 5, -27)	0.850	87.978(3, 0, -115)	0.923	173.973(3, 3, -56)	0.923
122.770(1, 2, -33)	0.507	85.979(2, 0, -83)	0.844	251.631(2, 6, -27)	0.843	88.642(3, 0, -114)	0.920	177.089(3, 3, -55)	0.919
126.783(1, 2, -32)	0.503	87.005(2, 0, -82)	0.839	258.065(2, 6, -26)	0.921	89.426(3, 0, -113)	0.919	180.462(3, 3, -54)	0.920
131.038(1, 2, -31)	0.504	88.122(2, 0, -81)	0.841	262.090(2, 6, -25)	0.847	90.259(3, 0, -112)	0.919	183.642(3, 3, -53)	0.926
135.062(1, 2, -30)	0.516	89.156(2, 0, -80)	0.851	272.306(2, 6, -24)	0.842	91.077(3, 0, -111)	0.920	186.137(3, 3, -52)	0.929
138.470(1, 2, -29)	0.537	89.961(2, 0, -79)	0.855			91.802(3, 0, -110)	0.922	189.156(3, 3, -51)	0.921
142.601(1, 2, -28)	0.576	90.967(2, 0, -78)	0.841	60.086(3, 0, -171)	0.917	92.496(3, 0, -109)	0.921	192.937(3, 3, -50)	0.919
145.615(1, 2, -27)	0.823	92.189(2, 0, -77)	0.837	60.402(3, 0, -170)	0.917	93.320(3, 0, -108)	0.919	196.957(3, 4, -50)	0.920
148.732(1, 3, -27)	0.535	93.447(2, 1, -77)	0.838	60.736(3, 0, -169)	0.917	94.228(3, 0, -107)	0.918	200.446(3, 4, -49)	0.928
154.508(1, 3, -26)	0.506	94.558(2, 1, -76)	0.843	61.104(3, 0, -168)	0.917	95.152(3, 0, -106)	0.919	202.351(3, 4, -48)	0.928
160.808(1, 3, -25)	0.506	95.478(2, 1, -75)	0.841	61.488(3, 0, -167)	0.917	96.017(3, 1, -106)	0.920	205.527(3, 4, -47)	0.930
166.873(1, 3, -24)	0.524	96.685(2, 1, -74)	0.835	61.870(3, 0, -166)	0.917	96.769(3, 1, -105)	0.921	208.233(3, 4, -46)	0.931
171.996(1, 3, -23)	0.600	98.085(2, 1, -73)	0.834	62.227(3, 0, -165)	0.917	97.597(3, 1, -104)	0.919	212.184(3, 4, -45)	0.921
176.529(1, 3, -22)	0.795	99.512(2, 1, -72)	0.834	62.565(3, 0, -164)	0.917	98.564(3, 1, -103)	0.918	217.025(3, 4, -44)	0.920
180.413(1, 4, -22)	0.574	100.745(2, 1, -71)	0.834	62.928(3, 0, -163)	0.917	99.587(3, 1, -102)	0.918	222.101(3, 4, -43)	0.921
188.195(1, 4, -21)	0.508	101.779(2, 1, -70)	0.834	63.327(3, 0, -162)	0.917	100.590(3, 1, -101)	0.918	226.755(3, 5, -43)	0.928
197.617(1, 4, -20)	0.511	103.176(2, 1, -69)	0.833	63.740(3, 0, -161)	0.917	101.462(3, 1, -100)	0.919	230.385(3, 5, -42)	0.929
206.042(1, 4, -19)	0.807	104.775(2, 1, -68)	0.834	64.147(3, 0, -160)	0.917	102.291(3, 1, -99)	0.918	234.691(3, 5, -41)	0.933
209.377(1, 4, -18)	0.654	106.364(2, 1, -67)	0.835	64.526(3, 0, -159)	0.917	103.302(3, 1, -98)	0.917	236.404(3, 5, -40)	0.941
219.395(1, 5, -18)	0.522	107.611(2, 1, -66)	0.841	64.889(3, 0, -158)	0.917	104.414(3, 1, -97)	0.916	241.499(3, 5, -39)	0.920
229.253(1, 5, -17)	0.544	108.852(2, 1, -65)	0.839	65.284(3, 0, -157)	0.917	105.515(3, 1, -96)	0.915	247.844(3, 5, -38)	0.920
238.302(1, 5, -16)	0.793	110.550(2, 1, -64)	0.837	65.716(3, 0, -156)	0.917	106.425(3, 1, -95)	0.913	254.230(3, 5, -37)	0.923
243.548(1, 6, -16)	0.654	112.381(2, 1, -63)	0.839	66.161(3, 0, -155)	0.917	107.278(3, 1, -94)	0.914	259.605(3, 6, -37)	0.929
256.815(1, 6, -15)	0.519	114.043(2, 1, -62)	0.853	66.596(3, 0, -154)	0.917	108.387(3, 1, -93)	0.915	264.803(3, 6, -36)	0.926
269.995(1, 6, -14)	0.884	115.304(2, 1, -61)	0.856	66.998(3, 0, -153)	0.917	109.553(3, 1, -92)	0.916	267.478(3, 6, -35)	0.957
		117.013(2, 1, -60)	0.842	67.389(3, 0, -152)	0.917	110.504(3, 1, -91)	0.918	272.259(3, 6, -34)	0.921
60.415(2, 0, -120)	0.833	119.068(2, 1, -59)	0.839	67.822(3, 0, -151)	0.917	111.412(3, 1, -90)	0.919		

TABLE 7
 COMPARISONS OF RESULTS OF THE MULTIPLETS IN TABLE 2. ν^{obs} DENOTES THE OBSERVED FREQUENCIES IN μHz , ν^{theo} DENOTES THE CALCULATED
 FREQUENCIES IN μHz . $\Delta\nu = |\nu^{\text{obs}} - \nu^{\text{theo}}|$

Multiplet	ID	ν^{obs} (μHz)	ν^{theo} (μHz)	$\Delta\nu$ (μHz)	Multiplet	ID	ν^{obs} (μHz)	ν^{theo} (μHz)	$\Delta\nu$ (μHz)
	f_{10}	106.152	106.024(1, -1)	0.128		f_{18}	122.559	123.228(2, -2)	0.669
1	f_{12}	110.637	110.476(1, 0)	0.161	11	f_{28}	144.934	144.904(2, +1)	0.030
	f_{14}	115.036	114.928(1, +1)	0.108		f_{42}	194.179	194.638(2, -2)	0.459
	f_{31}	162.625	162.360(1, -1)	0.265	12	f_{47}	216.758	216.547(2, +1)	0.211
2	f_{34}	167.007	166.873(1, 0)	0.134		f_{48}	222.367	222.005(2, -2)	0.362
	f_{35}	171.485	171.386(1, +1)	0.099	13	f_{51}	252.079	251.871(2, +2)	0.208
	f_{41}	192.909	193.216(1, -1)	0.307		f_{22}	125.296	125.696(3, -1)	0.400
3	f_{43}	197.503	197.617(1, 0)	0.114	14	f_{24}	133.453	133.602(3, 0)	0.149
	f_{44}	201.898	202.018(1, +1)	0.120		f_{27}	141.765	141.508(3, +1)	0.257
	f_5	87.275	86.767(1, -1)	0.508		f_{15}	115.706	116.152(3, -2)	0.446
4	f_6	96.149	95.707(1, +1)	0.442	15	f_{20}	123.812	124.093(3, -1)	0.281
	f_8	100.779	100.560(2, -2)	0.219		f_{17}	117.666	118.118(3, -3)	0.452
5	f_{11}	108.372	107.932(2, -1)	0.440	16	f_{25}	134.071	133.964(3, -1)	0.107
	f_{16}	115.872	115.304(2, 0)	0.568		f_{49}	233.083	233.576(3, -1)	0.493
	f_9	102.072	102.510(2, -2)	0.438	17	f_{50}	249.725	249.422(3, +1)	0.303
6	f_{21}	124.571	124.264(2, +1)	0.307		f_{26}	134.762	135.456(3, 0)	0.694
	f_{23}	132.028	131.516(2, +2)	0.512	18	f_{30}	158.977	159.148(3, +3)	0.171
	f_2	65.541	65.633(2, -2)	0.092		f_1	64.936	65.120(3, -1)	0.184
7	f_3	72.978	72.807(2, -1)	0.171	19	f_7	96.938	96.675(3, +3)	0.263
	f_{32}	164.262	164.281(2, -2)	0.019		f_{19}	122.769	122.827(3, -1)	0.058
8	f_{36}	171.638	171.635(2, -1)	0.003	20	f_{29}	155.380	154.588(3, +3)	0.792
	f_{33}	164.855	164.831(2, 0)	0.024		f_{38}	176.285	177.108(3, -2)	0.823
9	f_{37}	172.243	172.143(2, +1)	0.100	21	f_{46}	209.708	208.766(3, +2)	0.942
	f_{39}	189.056	188.534(2, 0)	0.522					
10	f_{45}	203.652	203.106(2, +2)	0.546					

TABLE 8
 POSSIBLE MODE IDENTIFICATIONS FOR THE UNIDENTIFIED OBSERVED FREQUENCIES BASED ON THE OPTIMAL MODEL. $\Delta\nu = |\nu^{\text{obs}} - \nu^{\text{theo}}|$.

ID	ν^{obs} (μHz)	$\nu^{\text{theo}}(l, n_p, n_g, m)$ (μHz)	$\Delta\nu$ (μHz)
f_{13}	112.291	112.212(0,1,0)	0.079
f_4	76.363	76.394(1,0,-51,-1)	0.031
		76.303(2,0,-117,+2)	0.060
f_{40}	190.612	190.803(2,3,-39,+2)	0.191
f_{52}	262.964	262.382(1,6,-14,-1)	0.582